Flame-controlling continuation method for extinction of counterflow sooting flames with detailed chemistry

Erica Quadarella*[1], Junjun Guo†[1], Alberto Cuoci ‡[2], and Hong G. Im §[1]
[1]*Clean Combustion Research Center, King Abdullah University of Science and Technology, Thuwal 23955-6900, Saudi Arabia*
[2]*CRECK Modeling Lab, Politecnico di Milano, Milano 20133, Italy*

The generation of S-curves for the extinction of counterflow sooting flames has been accomplished by implementing a flame-controlling continuation method inclusive of soot model. The code can generate solutions for augmented flamelets databases, including soot scalars, useful for Flamelet Progress Variable (FPV) tabulations for sooting turbulent simulations. Indeed, the inclusion of all S-curve's branches brings substantial improvements in the reproduction of extinction/re-ignition regimes or flame/acoustic interactions. In this context, developing a reliable tool for S-curve generation, with coupled reproduction of gas-phase and soot characteristics, is of great importance. The algorithm calculates the flamelet states through a 2-point flame-controlling continuation method with control on species mass fractions. Soot calculation is coupled with gas kinetics at every continuation so that flamelet states are inclusive of soot formation effects on precursors' consumption and flame temperature. The flame and soot features can be correctly predicted along the whole curve with smooth transitions between branches. A brief introduction on general S-curve properties is given, using the implementation on hydrogen flames with different oxidizer's inlet temperatures. Besides, soot characteristics are thoroughly investigated on ethylene flames at different pressures.

I. Nomenclature

a	=	strain rate
P'	=	uniform pressure curvature
P	=	pressure
L	=	distance between nozzles
T	=	temperature
U	=	scaled momentum
v	=	velocity
Y	=	mass fraction
x	=	spatial coordinate
Z	=	mixture fraction
ρ	=	density

II. Introduction

Primitive variable approaches represent an effective way to include the turbulence-chemistry interaction in Large Eddy Simulations (LES) or Reynolds-averaged Navier Stokes (RANS) simulations of turbulent reactive flows. Starting from the assumption that the flame front structure of a turbulent flame is locally equivalent to that of laminar flames, namely flamelets, the latter are generated as look-up tables. This can be done through counterflow flames, describing the different flamelet states at varying strain rate. However, chemistry makes the problem strongly non-linear, yielding multiple solutions. More specifically, the flame response can be read in the so-called S-curve, where a flame feature, e.g.

*PhD student, CCRC KAUST, erica.quadarella@kaust.edu.sa
†Research Scientist, CCRC KAUST, junjun.guo@kaust.edu.sa
‡Professor, CRECK modeling Lab, alberto.cuoci@polimi.it
§Professor, CCRC KAUST, hong.im@kaust.edu.sa, AIAA Associate fellow.

the maximum temperature or some reaction product, is expressed as a function of the strain rate or scalar dissipation rate. In such representation, three main regions can be distinguished: an upper branch, representing the fully burning solution, a middle one, depicting unstable conditions, and finally, a lower branch, characterised by weakly burning solutions. The different branches are connected by turning points, whose characterisation is usually complex due to the singularity of the Jacobian matrix in that region. Similarly, the estimation of the middle branch requires particular attention from a numerical point of view: indeed, for a fixed strain rate, a small perturbation leads to the corresponding stable solution. The importance of including the whole curve in the flamelets set is of practical relevance in extinction/re-ignition regimes [1] as well as for flame/acoustic interactions [2, 3].

The formation of soot usually adds complexity to the adoption and computation of flamelet states. Indeed, because of its long characteristic formation times [4] soot is not able to respond instantaneously to progress variables, requiring the adoption of augmented flamelet databases, with the inclusion of soot scalars beyond the thermochemical state. Also, due to the strong sensitivity of soot to strain rate, an accurate description of all flamelet states is essential to predict its production at varying flow residence times faithfully.

This work aims to formulate and implement a flame-controlling continuation method for S-curve generation with the inclusion of soot production/consumption in counterflow flames. The proposed methodology, as well as the inclusion of the soot module, are presented and discussed. The implemented code is then tuned and employed to discuss general S-curve properties on hydrogen counterflow flames, while soot scalars behaviour is assessed on ethylene flames at different pressures.

III. Numerical method

A. Flame-controlling continuation method

The computation of flamelet states for the whole S-curve is usually achieved through the arclength [5] or flame-controlling [6] continuation methods. While the first one represents an effective way to generate the curve, its implementation might result particularly complex. For this reason, Nishioka et al. [6] developed a flame-controlling continuation method in the attempt to conceive a more accessible but valid alternative to the arclength method.

In the flame-controlling continuation method, the computation of different flamelets states is achieved by controlling a scalar value of the flame profile, with a new solution calculated to be close enough to the previous one, taken as a first guess. The idea is to obtain the strain rate as an output of the flame calculation. This is done by getting rid of one boundary condition on either v_f or v_{ox} and introducing a new internal condition on either the temperature or the mass fraction of combustion products, including radicals. This method is also called 1-point continuation. However, the authors showed that this approach encounters difficulties determining the first turning point between the upper and middle branches. For this reason, a more stable version of the method can be achieved through a 2-point continuation, where both boundary conditions on velocities are removed, and another internal condition is added.

B. Implementation in OpenSMOKE++ with the inclusion of soot

OpenSMOKE++ [7] is an extensively validated numerical framework for simulations of reacting systems with detailed kinetic mechanisms. It has been widely used to compute counterflow flames, including flame configurations leading to sooting conditions [8]. Therefore, it represents a useful framework for establishing a continuation method for sooting flames in flamelets generation. The soot models in OpenSMOKE++ vary from the sectional [9], accurate but computationally expensive, to the method of moments, more specifically the hybrid method of moments (HMOM) [10], which gives information on the mean values of the number density function (NDF) rather than the whole distribution, at an affordable computational cost. Although the continuations can be used with any soot model, the latter needs to resemble the one used in turbulent conditions. Therefore, as the computational cost is significantly reduced with the method of moments, results are presented in this work using the HMOM.

A 2-point continuations method is implemented in OpenSMOKE++ with control on species' mass fractions. Although temperature usually constitutes a good candidate as representative of the thermo-chemical state of a system, its exponential variation with the Arrhenius' formulation makes its control complex, as it results susceptible to small variations. On the other side, the concentration of species mainly produced by the combustion process (H_2, H_2O as well as radicals like H and OH) can also be representative of the system under different strain rates, with a unique peak value and wideness of the curve depending on the position along the S-curve.

The two internal conditions read:

$$x = x^* : \quad Y_{cv} = Y_{cv}^*, \tag{1}$$

$$x = x^{**} : \quad Y_{cv} = Y_{cv}^{**}, \tag{2}$$

where x and Y_{cv} are, respectively, the spatial coordinate and the controlled variable; x^* and x^{**} are the points corresponding to the internal conditions while Y_{cv}^* and Y_{cv}^{**} are the values the controlled variable has to assume. As mentioned before, the introduction of two new internal coordinates implies the removal of two boundary conditions, in this case, $v(x = 0) = v_f$ and $v(x = L) = v_{ox}$. To ease the numerical process of setting the internal conditions, a new dummy equation is added to the system:

$$\frac{dU_f}{dx} = 0, \tag{3}$$

where U_f is a new variable, which in this case represents the scaled momentum ($\frac{\rho v}{2}$) at the fuel side. Being U_f independent of x, it is treated as an eigenvalue of system. Therefore, the internal conditions can be set using Eq. 3 and the uniform pressure curvature $P^{'}$, the latter being another eigenvalue of the problem [11], independent of x. The boundary conditions on species transport equations, originally specified through the total mass flux (accounting for diffusion and convection), are modified according to the new unknowns v_f and v_{ox}. Therefore, the coupling between the species and momentum equations is required at all times. The values assumed by the controlled variable in the two internal conditions are determined based on the previous solution (which serves as the first guess) and adding or reducing the value by a sufficiently small ΔY_{cv}, calculated as a percentage of the previously measured value at that point. The points at which the internal conditions must be set are usually chosen in a steep region of the species profile.

The gas-phase evolves according to the new set of equations. Once the solution of the new flamelet state has been found, the grid refinement can be carried out with no further manipulation of the internal conditions. Soot calculation is performed at the end of the refinement process. Soot inception occurs by heterogeneous physical collisions of Polycyclic Aromatic Hydrocarbons (PAHs) forming a dimer. Consequently, a sink term for PAHs needs to be considered. For this reason, as well as for soot radiation effect on flame temperature, the thermo-chemical state is recomputed, always considering the previously set internal conditions. All species, temperature and momentum equations need to be coupled at this stage. The process is iterated for the number of continuations needed to complete the whole S-curve.

IV. Results and discussion

Due to the simplicity of the mechanisms and consequent low computational cost, the implementation is first tuned on hydrogen counterflow flames at different oxidizer's inlet temperatures. These cases are also used to briefly introduce the operation of the code and general S-curve properties and verify the consistency of the results with previous studies. Besides, sooting ethylene flames at different pressures are employed to assess the behaviour of soot scalars at varying strain rates and along the different S-curve branches. Boundary conditions for all cases are summarized in Table 1.

Table 1 Boundary conditions for the investigated counterflow flames

	H_2 flames	C_2H_4 flames
T_f [K]	300	300
T_{ox} [K]	300, 950	300
X_f [-]	H_2=0.3, N_2=0.7	C_2H_4=0.35, N_2=0.65
X_{ox} [-]	Air	Air
P [atm]	1	1, 3, 5
L [cm]	2	2

Kinetics is solved using H_2 Polimi mechanism [12] for the hydrogen flames and a reduced version of Kaust-Aramco PAH 1.0 mechanism, containing 99 species and PAHs formation up to A7 [13], for the ethylene flames. Mixture averaged diffusion coefficients, Soret effect and radiation heat losses are considered in the gas phase.

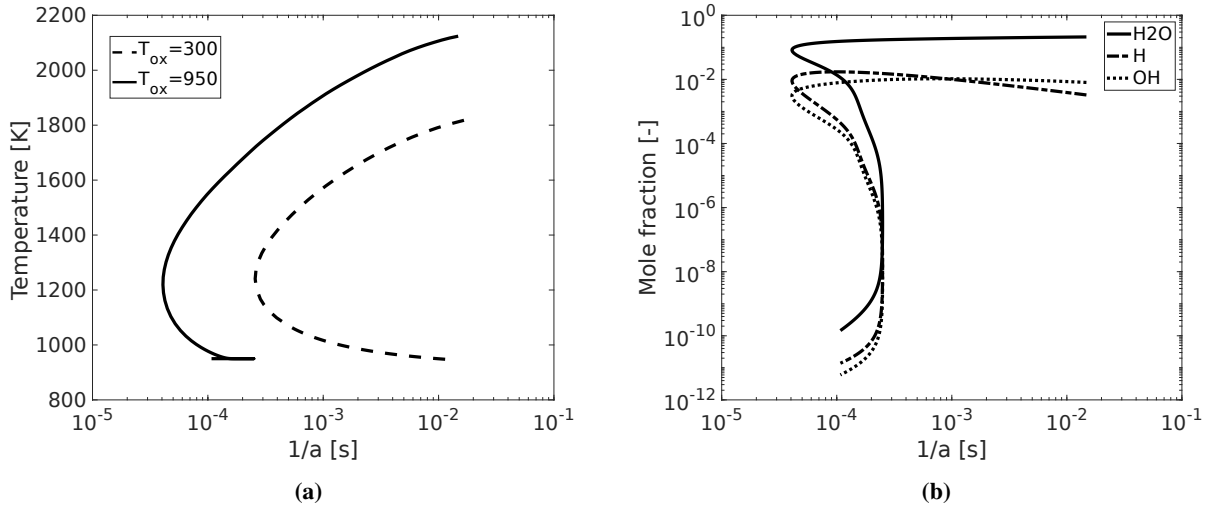

(a) **(b)**

Fig. 1 (a): S-curves for peak temperature as function of the inverse of strain rate for the H_2 cases with T_{ox} = 300 K and T_{ox} = 950 K; (b): S-curves for H_2O, H and OH species peak mass fractions as function of the inverse of strain rate for the H_2 case with T_{ox} = 950 K.

The variation of maximum temperature with the inverse of strain rate is shown in Fig.1a for hydrogen flames. Starting from a low strain rate point on the upper branch, which can be computed with the conventional counterflow code to initialize the procedure, the continuations proceed towards the first turning point, whose estimation might be critical, as a small variation on the internal conditions leads to a significant change on the whole flame configuration. The first turning point is also referred to as the extinction point, as it represents the higher strain rate at which the flame can sustain. The solution proceeds along the middle branch up to the point where temperature and the production of radicals are so small that the flame extinguishes. At the end of the middle branch, the second turning point, namely the ignition point, is only distinguishable for the flame with T_{ox} = 950 K, as it is above the ignition temperature. As pointed out by Nishioka et al. [6], in the temperature plot, the second turning point might be connected to the lower branch through a cusp (Fig.1a), which is another reason why controlling species mass fractions instead of temperature is preferred. Indeed, the S-shaped curve is better visualized in terms of species mass fractions, like H_2O, H and OH, reported in Fig.1b for the H_2 case with T_{ox} = 950 K. For these species, the transition between different branches appears smoother. More in general, the controlled variable can be arbitrarily chosen among reaction's products. Good candidates are those species whose profile changes monotonically with the strain rate. It is noticed that while maximum H_2O progressively decreases along the upper branch, the production of radicals like OH and H first increases and starts decreasing monotonically only along the middle branch. For this reason, H_2O was chosen as the controlled variable for this case. The location of the internal conditions should be chosen in a steep region of the controlled variable's profile to ensure good numerical convergence. This position can change with the proceeding of the continuations, as the profiles shrink and widen. The percentage increment/decrement of the internal condition value can also be arbitrarily chosen, but it should be kept around a few percentage points (2-3%) to ensure numerical convergence. In some critical regions, e.g. turning points or the tail of the middle branch, it might be necessary to work with 0.5-1% only.

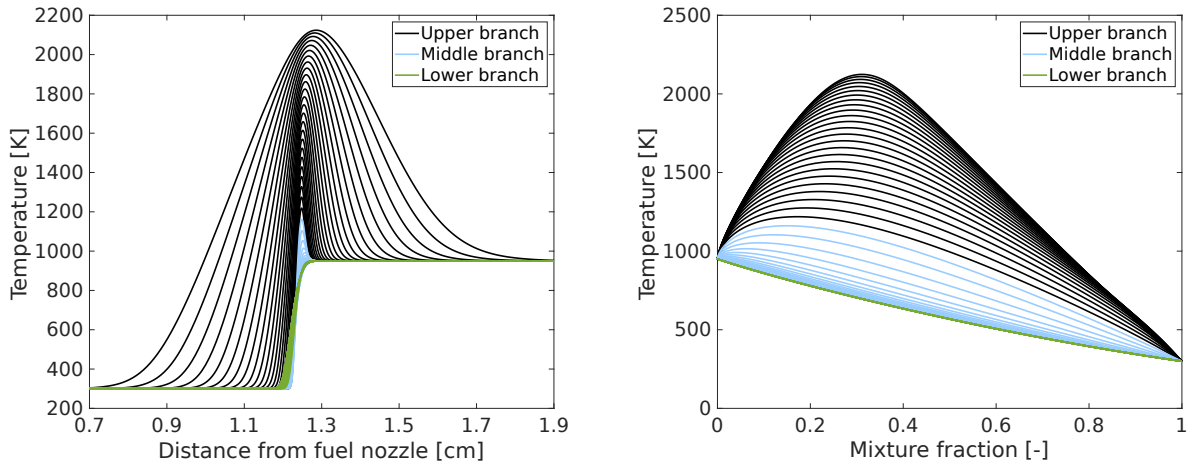

(a) **(b)**

Fig. 2 Temperature profiles evolution along continuations in the physical (a) and mixture fraction (b) spaces for the H_2 flame with T_{ox} = 950 K.

As this is a two-points continuation method, both the magnitude and the position of the profiles are controlled. Fig.2 shows the evolution of the temperature profile in the physical space, i.e. the distance between the two nozzles, and the mixture fraction space for all continuations for the H_2 case with T_0 = 950 K. In Fig.2a, the temperature profile, and consequently the flame thickness, progressively shrinks toward the first turning point, as a result of the increasing strain rate; it then tends to widen proceeding along the middle branch before shrinking again along the lower branch. If the same profiles are plotted in the mixture fraction space (Fig.2b), the transformations appear smoothed. In fact, as previously explained by Sung et al. [14], the physical dependence of the flame thickness on $1/\sqrt{a}$ is lost in the mixture fraction space. This makes mixture fraction a good candidate to effectively visualize the changes along the S-curves of any flame scalar.

The general characteristics of the S-curves on the hydrogen flames are found in agreement with previous studies [6, 15].

Ethylene flames are next analyzed to assess the behaviour of soot scalars along the S-curve. PAHs from A2 to A7 are included in the set of precursors. Thermophoresis is accounted for while radiation of soot particles is found to have negligible effect in this type of flames [8, 16], as temperature does not reach high values and the amount of soot formed does not exceed a few ppm, even at low strain rates. Fig.3 shows the S-curve of temperature, OH and A2 mole fractions, and dimerization rate for the C_2H_4 flames at 1, 3 and 5 atm, as a function of the inverse of strain rate. The temperatures reached in the upper branch (Fig.3a) becomes higher at increasing pressure, and the extinction point shifts to higher strain rates. Besides, the curves converge to similar values of maximum temperature along the middle branch, shifting the weakly reactive states toward lower strain rates with lower pressures. The OH radical (Fig.3b) maintains the shift of the extinction point, but it is found in a lower amount at increasing pressure, a direct consequence of recombination reactions favoured by pressure. The change of OH appears monotonic, especially on the middle branch, which endorses the adoption of such species as the controlled variable in this region. A2, namely naphthalene, is the smallest PAH considered in the set of precursors. Differently from OH, A2 is found to be highly affected by the strain rate (Fig.3c), with a difference between the low strain rate points on the upper branch and the extinction point that can reach a few orders of magnitude. This is expected since the characteristic chemical times of PAHs are known to be longer than those of typical combustion products, consequently being highly affected by flow residence times [17]. Also, pressure has the known effect of increasing PAHs production and soot formation, as experimentally and numerically found in many research works, on both laminar and turbulent flames [18–20]. The characteristics of the A2 S-curve are inevitably reflected onto the dimerization rate (Fig.3d), one of the soot scalars usually included in the tabulation process. Indeed, it gets to the minimum value at the first turning point region, where the combination of low residence times and temperature inhibits the formation of PAHs and, consequently, their propensity to form soot. Even though the temperature decreases along the middle branch, the longer flow residence times bring back the dimerization rate to higher values. The latter finally drops when the flame approaches the weakly reactive states, and temperature is

not sufficient anymore to sustain soot formation.

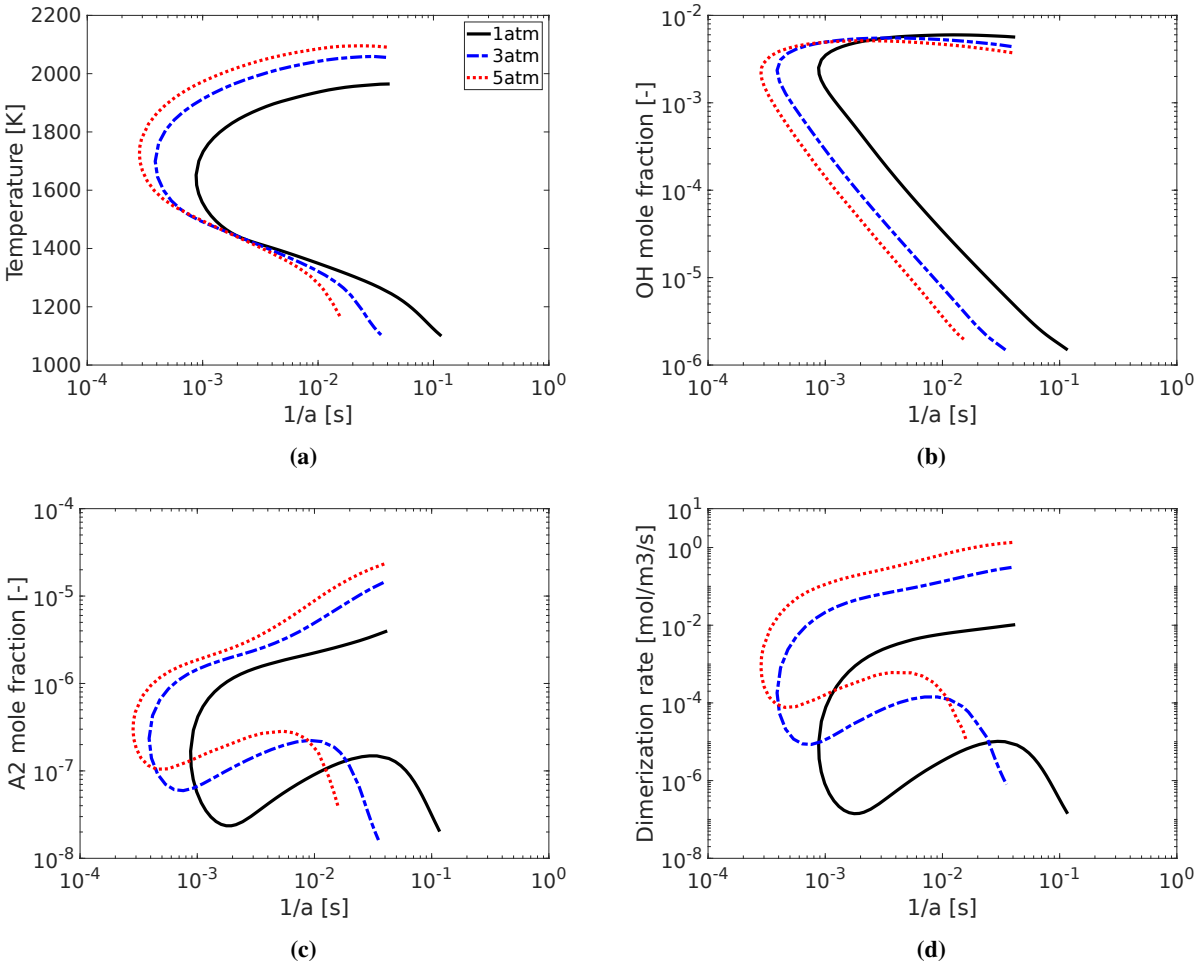

Fig. 3 S-curves for temperature (a), OH (b), A2 (c) and dimerization rate (d) as function of the inverse of strain rate for the C_2H_4 cases at different pressures.

Thanks to the coupling of gas and solid phases at all continuations, the effects of soot formation on the gas-phase are already accounted for in every flamelet solution. The generated S-curves can be employed in FPV approaches [21] that, differently from the traditional flamelets approaches, can cover all branches, exploiting the monotonicity of relevant quantities like temperature against a progress variable (Fig.4 with $C = max(Y_{H_2O} + Y_{CO_2})$).

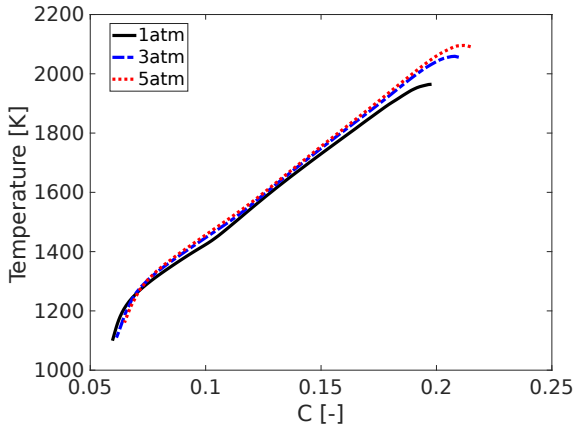

Fig. 4 Temperature peak against progress variable $C = max(Y_{H_2O} + Y_{CO_2})$ for the C_2H_4 cases at different pressures.

V. Conclusions

A 2-point flame-controlling continuation method has been successfully implemented in OpenSMOKE++ with the inclusion of a soot module at each step. The controlled variable chosen among the combustion products or radical species with an almost monotonic variation with strain rate effectively exploits the continuation method and obtains a good characterization of flamelet states with smooth transition between different branches. The implementation was employed on hydrogen flames with different oxidizer's inlet temperatures and led to a satisfactory description of general characteristics of the S-curve, in agreement with previous works. Besides, the behaviour of soot scalars was assessed in ethylene counterflow flames at different pressures. The coupling at each continuation of the soot module with the gas phase efficiently includes the effect of soot formation on the gas phase in terms of precursors consumption and flame temperature. PAH species are significantly affected by changes in strain rate, differently from other main combustion products or radicals that are almost exclusively function of temperature and pressure. Indeed, despite the progressive decrement of temperature, the increasing dimerization rate along the middle branch due to longer residence times suggests that soot formation can still play a role at those flamelet states, whose estimation should not be neglected. Finally, performance optimization leaves more room for improvement.

Acknowledgments

The work was sponsored by the King Abdullah University of Science and Technology (KAUST).

References

[1] Pitsch, H., Cha, C. M., and Fedotov, S., "Flamelet modelling of non-premixed turbulent combustion with local extinction and re-ignition," *Combustion Theory and Modelling*, Vol. 7, No. 2, 2003, pp. 317–332.

[2] Nguyen, T. M., and Sirignano, W. A., "The impacts of three flamelet burning regimes in nonlinear combustion dynamics," *Combustion and Flame*, Vol. 195, 2018, pp. 170–182.

[3] Ladeinde, F., and Lou, Z., "Improved flamelet modeling of supersonic combustion," *Journal of Propulsion and Power*, Vol. 34, No. 3, 2018, pp. 750–761.

[4] Cuoci, A., Frassoldati, A., Faravelli, T., and Ranzi, E., "Formation of soot and nitrogen oxides in unsteady counterflow diffusion flames," *Combustion and Flame*, Vol. 156, No. 10, 2009, pp. 2010–2022.

[5] Keller, H. B., and HB, K., "Numerical solution of bifurcation and nonlinear eigenvalue problems." *Applications of Bi- furcation Theory (P. Rabinowitz, Ed.)*, 1977.

[6] Nishioka, M., Law, C., and Takeno, T., "A flame-controlling continuation method for generating S-curve responses with detailed chemistry," *Combustion and Flame*, Vol. 104, No. 3, 1996, pp. 328–342.

[7] Cuoci, A., Frassoldati, A., Faravelli, T., and Ranzi, E., "OpenSMOKE++: An object-oriented framework for the numerical modeling of reactive systems with detailed kinetic mechanisms," *Computer Physics Communications*, Vol. 192, 2015, pp. 237–264.

[8] Pejpichestakul, W., Frassoldati, A., Parente, A., and Faravelli, T., "Soot modeling of ethylene counterflow diffusion flames," *Combustion Science and Technology*, Vol. 191, No. 9, 2019, pp. 1473–1483.

[9] Saggese, C., Ferrario, S., Camacho, J., Cuoci, A., Frassoldati, A., Ranzi, E., Wang, H., and Faravelli, T., "Kinetic modeling of particle size distribution of soot in a premixed burner-stabilized stagnation ethylene flame," *Combustion and Flame*, Vol. 162, No. 9, 2015, pp. 3356–3369.

[10] Mueller, M., Blanquart, G., and Pitsch, H., "Hybrid method of moments for modeling soot formation and growth," *Combustion and Flame*, Vol. 156, No. 6, 2009, pp. 1143–1155.

[11] Mittal, V., Pitsch, H., and Egolfopoulos, F., "Assessment of counterflow to measure laminar burning velocities using direct numerical simulations," *Combustion Theory and Modelling*, Vol. 16, No. 3, 2012, pp. 419–433.

[12] Creckmodeling, "Syngas (H2/CO) mechanism (Version 2003, March 2020)," , 2020. URL `http://creckmodeling.chem.polimi.it/`.

[13] Selvaraj, P., Arias, P. G., Lee, B. J., Im, H. G., Wang, Y., Gao, Y., Park, S., Sarathy, S. M., Lu, T., and Chung, S. H., "A computational study of ethylene–air sooting flames: Effects of large polycyclic aromatic hydrocarbons," *Combustion and Flame*, Vol. 163, 2016, pp. 427–436.

[14] Sung, C., Liu, J., and Law, C. K., "Structural response of counterflow diffusion flames to strain rate variations," *Combustion and Flame*, Vol. 102, 1995, pp. 481–492.

[15] Kreutz, T., Nishioka, M., and Law, C., "The role of kinetic versus thermal feedback in nonpremixed ignition of hydrogen versus heated air," *Combustion and flame*, Vol. 99, No. 3-4, 1994, pp. 758–766.

[16] Liu, F., Guo, H., Smallwood, G. J., and El Hafi, M., "Effects of gas and soot radiation on soot formation in counterflow ethylene diffusion flames," *Journal of Quantitative Spectroscopy and Radiative Transfer*, Vol. 84, No. 4, 2004, pp. 501–511.

[17] Cuoci, A., Frassoldati, A., Faravelli, T., and Ranzi, E., "Frequency response of counter flow diffusion flames to strain rate harmonic oscillations," *Combustion Science and Technology*, Vol. 180, No. 5, 2008, pp. 767–784.

[18] McArragher, J., and Tan, K., "Soot formation at high pressures: a literature review," *Combustion Science and Technology*, Vol. 5, No. 1, 1972, pp. 257–261.

[19] Guo, H., Gu, Z., Thomson, K. A., Smallwood, G. J., and Baksh, F. F., "Soot formation in a laminar ethylene/air diffusion flame at pressures from 1 to 8 atm," *Proceedings of the Combustion Institute*, Vol. 34, No. 1, 2013, pp. 1795–1802.

[20] Boyette, W. R., Bennett, A. M., Cenker, E., Guiberti, T. F., and Roberts, W. L., "Effects of pressure on soot production in piloted turbulent non-premixed jet flames," *Combustion and Flame*, Vol. 227, 2021, pp. 271–282.

[21] Pierce, C. D., and Moin, P., "Progress-variable approach for large-eddy simulation of non-premixed turbulent combustion," *Journal of fluid Mechanics*, Vol. 504, 2004, p. 73.